RSC Advances

ROYAL SOCIETY OF CHEMISTRY

www.rsc.org/advances

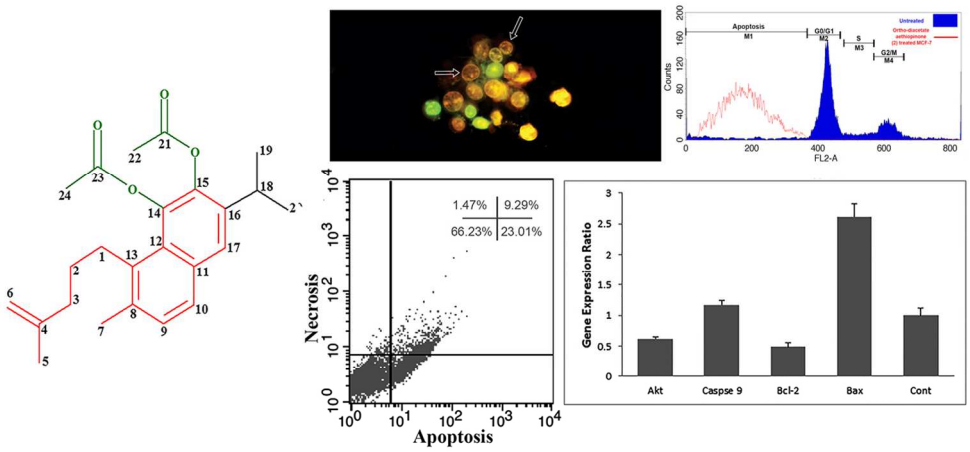

Ketoethiopinone (1) and Ortho-diacetate aethiopinone (2) were identified from the roots of S. sahendica and evaluated for their anti-cancer activity in MCF-7 breast cell lines. An effort was also made to determine the type of the MCF-7 cell death treated with 2, aiming to clarify the mechanism by which proliferation was limited.
119x57mm (300 x 300 DPI)

Abietane diterpenoid of *Salvia Sahendica* Boiss and Buhse potently inhibits MCF-7 breast carcinoma cells by suppression of PI3K/AKT pathway

Vala Kafil[a, b, c†], Morteza Eskandani[a, b†], Yadollah Omidi[a, c], Hossein Nazemiyeh[a, c]*, Jaleh Barar[a, c]**

[a] *Research Center for Pharmaceutical Nanotechnology, Tabriz University of Medical Sciences, Tabriz, Iran*

[b] *Student Research Committee, Faculty of Pharmacy, Tabriz University of Medical Sciences, Tabriz, Iran*

[c] *Faculty of Pharmacy, Tabriz University of Medical Sciences, Tabriz, Iran*

[†] ***These authors contributed equally to this work and should be considered as first authors.***

Corresponding authors:

* Hossein Nazemiyeh, Professor of Pharmacognosy, Nazemiyehh@tbzmed.ac.ir , Tel: +98 41 333367014, Fax: +98 41 33367929

** Jaleh Barar, Associate Professor of Biomedicine, jbarar@tbzmed.ac.ir, Tel: +98 41 33367914, Fax: +98 41 33367929

Abstract

In the current study, we report on the bioactive compounds isolated from the roots of *Salvia Sahendica* Boiss and Buhse using bioassay-guided procedures and their biological effects against MCF-7 breast carcinoma cells. In comparison with other solvents, the hexane-based extraction resulted in the most potent anti-cancer activity, and hence it was subjected to more phytochemical fractionation analyses using vacuum liquid chromatography (VLC), reversed-phase high pressure liquid chromatography (HPLC) and NMR spectroscopy. The biological impacts of the isolated pure compounds were evaluated using MTT, DAPI and acridine orange/ethidium bromide staining (AO/EB) assays. Cell cycle analysis was performed to assess the sub-G_1 population of the cells treated with the extracted compounds, while the FITC-labeled annexin V assay was used to study the apoptosis profile. The gene expression profile of the treated cells was studied by quantitative PCR, looking at key genes (*Caspase 9*, *Bax*, *Akt* and *Bcl-2*) involved in apoptosis. Ketoethiopinone (**1**) and ortho-diacetate aethiopinone (**2**) compounds were identified using ^{1}H and ^{13}C-NMR. Compounds **1** and **2** showed profound inhibitory impacts in the treated MCF-7 cells with the IC_{50} values of 8.6 and 14.2 µg/mL at 48 h, respectively. DAPI and AO/EB assays resulted in significant alternations in the nucleus through chromatin remodeling in the treated cells with somewhat impacts on the integrity of cell membrane. Annexin V flow cytometry assay revealed that the treated cells with the compound **2** resulted in early and late apoptosis (~30%). Gene expression profiling demonstrated significant ($p<0.05$) changes in the expression of *Bcl-2*, *Caspase 9*, *Bax* and *Akt* in the treated cell with the compound 2 with profound impacts on Bax and Akt pathways. Taken all, we propose ortho-diacetate aethiopinone as a new class of anticancer agents with great translational potential for clinical uses against solid tumors.

Keywords: *Salvia sahendica*, ortho-diacetate aethiopinone, Anti-cancer, Breast Cancer, MCF-7, Apoptosis, Necrosis

1. Introduction

Pursuant to the report of World Health Organization (WHO), breast cancer is the most common life-threatening malignancy in women, which caused about 13.7% of cancer deaths worldwide in 2008.[1]

Most patients with breast cancer require chemotherapy after initial surgery and radiotherapy modalities. Although the chemotherapy with potent anticancer agents inhibits the cancerous cells proliferation and growth, population of untouched cancerous cells remain resulting in recurrence of the disease. Further, these cells often show resistance to the chemotherapies via various mechanisms, which demands administrative of different anticancer agent In fact, majority of patients need multiple lines of therapy or alteration in the treatment protocol because of the occurrence of such resistancy in the cancerous cells to the chemotherapeutic agents. Resistance to the currently used chemotherapeutics in combating the breast cancer has highlighted our demands for novel anticancer agents, perhaps with minimal side effects yet maximal effectiveness against malignant cells.

Of various classes of anticancer agents, natural products such as sesquiterpenes, [2] steroids, polysaccharides, flavonoids, terpenoids and alkaloids have been the main source for development of a number of clinically important anticancer agents such as vincristine, vinbalstin and paclitaxel.

Salvia genus is the most common member of the *Labiatae* (Lamiaceae) family. It features conspicuously in the pharmacopoeias of different countries from the Far East to Europe. Different Salvia species have been used in a number of medical applications such as aromatization. *Salvia* species, especially *Salvia miltiorrhiza* , are considered as a source of anticancer compounds.[3]

Of a large number of *Salvia* species dispensed worldwide, almost 20 species are endemic of Iran.[4] *Salvia Sahendica* Boiss and Buhse is a known medicinal species of the Iran's Azerbaijan flour that its species names gives from its origin mountain; "Sahand". It has been traditionally used as antifungal and antibacterial herbal medicine, in addition to its application for management of dyspepsia.[5] Furthermore, various extracts of *S. sahendica* were found to impose anti-proliferative effect on the human melanoma and pancreatic cancer.[3]

Few studies have been reported upon phytochemical constituents extracted from different part of *S. sahendica*. For example, the extraction of sesquiterpene methylester, sclareol and salvigenin from the aerial parts has recently been reported.[6] Further, Jassbi et al and Fronza et al reported on the extraction of abietane diterpenoids (ferruginol and sahandinone) from the root parts of the plant.[3, 7] Beside, sahandinone, prionitin and horminon have been detected in the root of *S. sahendica*.[7] Some other important compounds have also been isolated from the root of *S. sahandica*, including: (a) sesterterpene 8α-Hydroxy-13-hydroperoxylabd-14,17-dien-19,16;23,6α-diolide, (b) salvileucolide-6,23-lactone, (c) norsesterterpene 17,18,19,20-Tetranor-13-*epi*-manoyloxide-14-en-16-oic acid-23,6α olide, (d) norambreinolide-18,6α-olide, and (e) 8α-Acetoxy-13,14,15,16-tetranorlabdan-12-oic acid-18,6α-olide.[8]

All these studies have highlighted the importance of *S. sahandica* as a source for some key compounds, however little is known about their biological activities in malignancies. Here in the current study, for the first time, we report on a bioassay-guided isolation and characterization of bioactive compounds of *S. sahandica* that imposed remarkable inhibitory effects on the human breast cancer cells.

2. Experimental

2.1. Material

MCF-7 cell line was purchased from Pasteur Institute (Tehran, Iran). RPMI Medium 1640, FBS, streptomycin and penicillin were provided from Gibco Invitrogen Corporation (Gibco, Invitrogen, UK). Pipettes, tissue culture flasks, 96 well plates, trypan-blue, and MTT were from Sigma–Aldrich (Sigma-Aldrich Co., Ltd., UK). RNX plus lysis buffer was purchased from CinnaGen (CinnaGen, Tehran, Iran). For the cDNA synthesis, Reverta-L reagent kit was used (Inter LabService, Russia). Hot Taq EvaGreen® qPCR Mix was used for the real time PCR (SinaClon Co, Tehran, Iran). DMSO and DAPI were from Merck (Darmstadt, Germany) and diethylpyrocarbonate (DEPC), Triton-X100 was purchased from Sigma-Aldrich Chemical Co. (Poole, UK). AnnexinV-FITC Kit, propidium iodide (PI), acridine orange and ethidium bromide were obtained from eBioscience (CA, San diego, USA). All other materials that are not mentioned were from Stratagene (La Jolla, CA, USA) and Fermentas Life Science (Burlington, Canada).

2.2. Plant material

Root parts of *Salvia sahendica* Boiss and Buhse, were gathered from the mountains of Tabriz-Basminj road, Iran in spring, 2012. The plant was identified by Professor Hossein Nazemiyeh, Head of the Herbarium at Tabriz University of Medical Sciences (TUOMS) and a voucher specimen (Tbz-FPh 736) representing the collection was deposited in the Herbarium at TUOMS, Tabriz, Iran. The plant root parts were dried at the room temperature while it was protected from the direct sunlight. Then, they were comminuted and kept in the closed containers at 2-8 °C.

2.3. Preparation of the extractions

Air dried powdered of the plant (200 g) were consecutively extracted by soxhlet using organic solvents including n-hexane (Hex), dichloromethane (DCM) and methanol. All the extraction solvents were evaporated *in vacuo* by rotary evaporator at an ambient temperature. Anti-proliferate properties of the extracts were evaluated using MTT cytotoxicity assay. The hexane-based extraction showed the highest cytotoxic effects, and hence was subjected to further fractionation using VLC.

2.4. Compounds isolation and identification

The Hex extract (3 g) was fractionated using VLC on a stationary phase of Merck Silica gel 60 GF_{254}, eluting with a gradient admixture of organic solvents including: Hex: Acetone (98:2, 96:4, 92:8, 90:10 ; 200 mL each), Hex: Acetone (80:20, 60:40, 40:60, 20:80, 0:100 ; 400 mL each), and finally Acetone: methanol (60:40, 50:50, 40:60, 30:70, 20:80, 10:90, 0:100 ; 300 mL each). The vacuum chromatography was repeated for 3 times to get enough amount of each fraction. The solvents of fractions were then removed under the circumstance of low pressure at 40°C. The yielded fractions were subjected to MTT assay, and the fractions with a dominant anti-

proliferate activity (eluted by 92-8%, 80-20%; Hex: Acetone) were further evaluated and fractionated using HPLC using designated systems and procedures.

2.5. Preparative HPLC

The fractions obtained by VLC were screened towards their cytotoxic impacts on the cultivated cells. Then, the designated fractions with the highest cytotoxic impacts were further isolated by preparative HPLC eluted with a linear gradient of acetonitrile (ACN)/water and monitored using a photo-diode-array detector at a range of 190 to 400 nm. For purification of 92:8% (Hex: acetone) fraction the most suitable HPLC program was set as system A(mobile phase: 0- 50 min, ACN from 70 to 90% in H_2O; 50-55 min, 90% ACN in H_2O; 55-56 min, ACN from 90 to 70% in H_2O; 56-62 min ACN 70% in H_2O, flow rate 20 mL/min. For 80:20% (Hex: acetone) fraction system B was developed as follows: mobile phase: 0-30 min, ACN from 60 to 70% in H_2O; 30-35 min, 70% ACN in H_2O; 35-45 min, ACN from 70 to 90% in H_2O; 45- 50 min ACN 90% in H_2O; 50-51 min, ACN from 90 to 60% in H_2O; 51-60 min, ACN 60% in H_2O, flow rate 20 mL/min. Then, the solvents of eluted fractions were removed by the rotary evaporator *in vacuo.* All the collected sub-fractions were monitored on TLC plates and the similar compounds were integrated. Once again, the cytotoxicity effects of the fractions were evaluated by MTT assay and the most potent anti-proliferate fractions were selected for the chemical structure determination and further biological investigations.

2.6. Determining the chemical structures

The structure of purified compounds were elucidated by UV-visible, ^{1}H-NMR and ^{13}C-NMR spectroscopy techniques. For ^{1}H-NMR and ^{13}C-NMR spectroscopy the sufficient amount of yielded compounds were dissolved in deuterated chloroform.

2.5. Cell culture and treatments

MCF-7 cells were cultured in Roswell Park Memorial Institute medium (RPMI) 1640 medium, containing 1% penicillin/streptomycin and 10% FBS in a humidified incubator (5% CO_2-95% air atmosphere) at 37°C. Various concentrations of the compounds ranging from 5-100 µg/mL were prepared in RPMI containing DMSO as co-solvent (not more than 0.3%) and 10% FBS. Subsequently, prior to treatments the serial dilutions were sterilized by filtration methods using 0.22 µm syringe filter (JET BIOFIL, Interlab Ltd, New Zealand)

2.6. Cell viability

MTT cytotoxicity assay was frequently used to measure the cell proliferation/viability and the mitochondrial activity. Mitochondrial NAD (P) H-dependent cellular oxidoreductase enzymes may reflect the number of viable cells present. These enzymes are capable of reducing the tetrazolium dye MTT 3-(4, 5-dimethylthiazol-2-yl)-2,5-diphenyltetrazolium bromide to its DMSO slouble formazan, which has a purple color. Thus, UV absorbance of the respective color may effectively show the extent of the viable cells. The MTT assay was performed for the cytotoxicity exclusion of the extracts, fractions and pure compounds in MCF-7 cells as reported previously.[9, 10] In this study, cells were cultivated at a density of 3.0×10^4 cells/cm^2 in 96-well plates and incubated at 37°C with a humidified atmosphere and allowed to attach overnight. At

70% confluency, the medium was substituted with a designated amount of the selected compound (as 200 μL of 5-100 mg/mL) and the cells were incubated over different time periods (i.e., 24, 48 and 72 h). After such incubation period, 20 μL/well of MTT solution in PBS (5 mg/mL, pH 7.4) was added and the cells were incubated at 37°C for 4 h in dark. Therefore, the media/MTT mixtures were replaced by 200 μL of DMSO containing 25 μL Sorenson's glycine buffer (0.1 M NaCl, 0.1 M glycine, pH 10.5). The absorbance of dissolved formazan crystals was determined spectrophotometrically at a wavelength of 570 nm using a Bioteck microplate reader (BioTek Instruments, Friedrichshall, Germany).

2.7. Cell morphology and nuclear staining

2.7.1. *Morphological Assessment*

After incubation with compounds for 24 h, the cells were monitored for any morphological alternations and detachment using Olympus IX81 fluorescence microscope (Olympus optical Co., Ltd. Tokyo, Japan) equipped with XM10 monochrome camera (Olympus, Hamburg, Germany).

2.7.2. *DAPI Staining*

For the nuclei condensation and fragmentation studies, the treated and untreated cells after 24 h incubation were fixed in 4% paraformaldehyde for 2 h, washed with PBS and then stained by DAPI.[11, 12] After washing with PBS, the cells were permeabilized by embedding in 0.1% Triton-X-100 for 5 min. Afterword, the cells were exposed to DAPI (final concentration 0.2 mg/mL) in

darkness for 5 min. Finally, using fluorescent microscopy, the morphology of the cells were investigated for possible changes in the pattern of nucleus and the remodeling of chromatin.

2.7.3. *Acridine Orange and Ethidium Bromide*

Apoptosis occurrence was further verified, morphologically after staining the cells with acridine orange and ethidium bromide (AO/EB) by a fluorescence microscopy as described previously.[13] Briefly, after 24 h incubation of the MCF-7 with different compounds, treated cells, were rinsed in PBS and exposed to the 50 µL of acridine orange/ethidium bromide solution (100 µg/mL of acridine orange and 100 µg/mL of ethidium bromide in PBS). Microscopic analyses were performed directly subsequent to dyes adding to the cells.

2.8. Apoptosis detection and quantification

2.8.1. *Cell cycle analysis*

Cell cycle analysis was performed to assess the sub-G_1 population of the cells treated with 20 µg/mL of the compounds for 24 h. Briefly, the cells were harvested with trypsin, centrifuged and washed (3×) with PBS. The cells were then resuspended and fixed with 1.0 mL ice cold ethanol (70%), and the samples were stored at 4°C for 30 min. For the staining of the cells, they were washedwith PBS (3×) by centrifugation at 850 ×g. To avoid the inadvertent staining of ds RNA and also to solely stain DNA, the cells were treated with 50 µL ribonuclease A at 37°C for 30 min. Next, the samples were washed and stained with propidium iodide at the final concentration of 5 µg/mL PI dissolved in PBS. Flow cytometry analysis was carried out for 10,000 events per cell sample through FL2-A band-pass filter (Propidium iodide) using Becton Dickinson (BD)

fluorescence-activated cell sorting (FACS) flow cytometer, FACScalibar (San Jose, CA, USA To analyze the fluorescence of the cell population(s), we used the freely available WinMDI 2.8 software (http://facs.scripps.edu/).

2.8.2. *Annexin V detection of apoptosis*

To find out the stage of the apoptosis/necrosis in the treated cells, the Annexin V flow cytometry analysis was performed as described previously.[14, 15] It should be stated that the annexin V is a phospholipid-binding protein with high affinity for phosphatidylserine, which translocate from the inner sheet to the external cell surface concurrent with early apoptosis event. In this study, annexinV-fluorescein isothiocyanate (FITC) apoptosis detection kit (BD science) was used following the manufacturer's protocol. Briefly, the treated cells were detached by gentle trypsinization and a total of 1.5×10^6 cells were washed (2×) with 1X binding buffer. Then, the cells were resuspended in 100 µL binding buffer containing 5 µL annexin V. Subsequent to incubation in the dark at room temperature for 20 min, 5 µL PI were added to the samples, which were analyzed in comparison with the untreated cells as negative control using BD FACScalibur flow cytometer (San Jose, CA, USA) and WinMDI 2.8 software.

2.9. Quantitative PCR

The cultivated cells treated with compound 2 (60 µg/mL for 24 h) were further subjected to the gene expression profiling. Total RNA was extracted by RNXplus lysis buffer according to the manufacturers' protocol.[16] The quantity and quality of the isolated RNA was evaluated using a NanoDrop® ND-1000 Spectrophotometer (Nano-Drop Technologies, Wilmington, DE, USA)

and RNA gel electrophrosis. The reverse transcription reaction was carried out using an AmpliSens® Leukosis-Quantum M-bcr-FRT PCR kit. Briefly, 10 µL of RNA-samples were added to the appropriate test tube containing 10 µL of ready-to-use reagent mix (6 µL of Revertase (MMlv), 5 µL of RT-G-mix-1 and RT-mix) and incubated at 37°C for 30 min using an Astec thermal cycler PC-818 (Astec, Fukuoka, Japan).

The qPCR reactions were carried out in a total volume of 20µL using Bio-Rad iQ5 multicolor thermal cycler (Bio-Rad, Inc., Hercules, CA, USA). Each well contained: 1 µL primer (10 pmol/µL each primer) (Table 1), 1 µL cDNA, 4 µL of 5X HotTaq EvaGreen qPCR Mix and 16 µL DNAse/RNAse free DEPC treated water. The thermal cycling conditions for the real time PCR were as following: 94°C for 10 min, 40 cycles of 95°C for 15 sec, 55-61°C for 1 min, and 72°C for 30 sec.

Analyses of the results were performed by the Pfaffl technique and the closure times (CTs) were normalized to the expression of 1*8S* rRNA as a housekeeping gene.[17] All reactions were accomplished as triplicates with internal positive and negative controls.

*****Table 1*****

2.10. Statistical analysis

Data obtained from the assays were analyzed by either Student's t-test or One-Way ANOVA using SPSS 11.0 software (Statistical Package for the Social Sciences 11.0) followed by a *post-hoc* multiple comparison analysis. A p value less than 0.05 was considered for the statistical significance. Data presented in this study are replicative of 3-4 experiments.

3. Results and discussion

3.1. Determining the chemical structures

This study was planned to evaluate the bioactive compounds isolated from the root of *S. sahendica.* To pursue this aim, a bioassay-guided isolation and fractionation platform was recruited. The purified compounds were characterized by UV/vis, and ^{1}H- and ^{13}C-NMR spectroscopies, and also compared with previously reported structures. As shown in Fig.1, the phytochemical analyses of the compounds led to the isolation of two abietane diterpene compounds (ketoethiopinone (**1**) and ortho-diacetate aethiopinone (**2**)) which showed anti-proliferative properties.

***** Fig. 1*****

Ketoethiopinone (**1**) is a known abietane diterpene that has been recognized and elucidated from the roots of *Salvia aethiopis*[18] and *Salvia argentea.*[19] To the best of our knowledge, this is the first report on ketoethiopinone existence in the roots of *S. sahendica*. Using preparative HPLC separation method, an amorphous red residue was obtained after evaporation of the excess solvents *in vacuo.* The compound (**1**) displayed λ_{max} (online) at 244, and 337 nm which were in well-consensus with the presence of an orthoquinone moiety in (**1**).[18] In the first evaluation, according to the ^{13}C-NMR results together with the number of detected carbon, a diterpene structure has been proposed for (**1**). Occurrence of three characteristic peaks at δ 200.72, 184.42 and 182.64 proposed three carbonyl groups in the structure of (**1**). Also, existence of a typical peak at δ 110.64 in C-NMR and δ 4.89 (2H, bs, H_6) in ^{1}H-NMR suggested one exocyclic double bond. ^{1}H-NMR spectrum of (**1**) also showed the presence of one aromatic methyl group at δ 2.23 (3H, s, H_7), an isopropyl group with signals at δ 1.11 (6H, d, J=6.74, H_{19-20}) and a methine septet at δ 2.98 (H, m, H_{18}).

Ortho-diacetate aethiopinone (**2**) has previously been reported by boya *et al.*[18] However, there is no sufficient evidence in relation with compound (**2**) elucidation from the other sources. To the best of our knowledge, our study is the first report on the presence of ortho-diacetate aethiopinone in the root of *S. sahendica*. The ^{1}H-NMR spectrum of (**2**) preserved the same pattern of aromatic signals observed for compound (**1**). The remaining signals were as same as ketoethiopinone, with an exception upon two more aliphatic methyl groups that appeared as singlet peaks in δ 2.33 (3H,s, H_{24}) and 2.31 (3H,s, H_{22}). Also, a prominent peak corresponding the carbonyl group in the ^{13}C-NMR spectrum of (**1**) was not observed in the spectrum of (**2**). Further, in compound (**2**), two carbonyl groups were observed as characteristic peaks in δ 181.18 (C21), 180.31(C23), which seemed to be shifted towards the low magnetic field as compared to (**1**). Beside, as compared to the ^{13}C-NMR data of (**1**), , there were two more aromatic carbon signals in δ 134.15 and 146.91 in compound (**2**), respectively corresponding the (C14) and (C15).

3.2. Chromatographic and spectroscopic data

3.2.1. *Ketoethiopinone (**1**)*

Red amorphous solid ; Rt: 7.30 min (purified by the system A chromatography); ^{1}H-NMR ($CHCl_3$-d_4, δ/ppm, J/Hz): 7.06 (1H, d, J=8.3, H_{10}), 6.97 (1H, d, J=8.5, H_9), 6.89 (H, s, H_{17}), 4.89 (2H, bs, H_6), 2.91-2.98 (H, m, H_{18}), 2.59-2.70 (2H,m, H_2), 2.23(3H, s, H_7), 2.02 (3H,s,H_5), 1.80-1.86 (2H, m, H_3), 1.11 (6H, d, J=6.74, $H_{19\text{-}20}$). ^{13}C-NMR ($CHCl_3$-d_4, δ/ppm, J/Hz): 200.72 (C1), 184.42 (C14), 182.64 (C15), 149.75 (C4), 148.17 (C9),140.00 (C8), 138.22 (C16), 136.26 (C13),

134.56 (C11), 129.10 (C10), 125.51 (C17), 110.64 (C6), 44.77 (C3), 44.68(C2), 24.94 (C18), 20.48 (C5), 20.34(C7), 18.71 (C19-C20).

3.2.2. *Ortho-diacetate aethiopinone (**2**)*

Red gum; Rt: 9.25 min (purified by the system B chromatography); ^{1}H-NMR ($CHCl_3$-d_4, δ/ppm, J/Hz): 7.3 (1H, d, J=7.64, H_{10}), 7.05 (1H, s, H_{17}), 6.99 (1H, dd, J=7.59, 1.3, H_9), 4.67 (2H, br.s, H_6), 2.91-3.01 (3 H, m, H_l, H_{18}), 2.33 (3H,s, H_{24}), 2.31 (3H,s, H_{22}), 2.08-2.20 (2H, m, H_3), 1.66-1.77 (2H,m,H_2), 1.58 (3H,s,H_5), 1.11 (6H,d, J=6.8,H_{19}, H_{20}).^{13}C-NMR ($CHCl_3$-d_4, δ/ppm, J/Hz): 181.18 (C21), 180.31(C23), 147.47 (C4), 146.91 (C15), 144.43(C13), 143.25 (C16), 139.05 (C8), 135.56 (C10), 134.15 (C14), 131.14 (C11), 126.90 (C17), 122.61 (C12), 118.16 (C9),108.97(C6) 37.23(C3), 29.30 (C1), 25.65(C2), 25.40(C18), 24.60(C19-C20), 21.36(C5), 21.25(C22), 18.77(C7), 16.44(C24).

3.3. Cytotoxic effects on MCF-7 cells

The cytotoxic effects of the compounds on MCF-7 cells were evaluated by MTT cytotoxicity assay. As shown in Fig. 2, compounds (**1**) and (**2**) were able to induce cytotoxicity in the treated cells in a time- and dose-dependent manner, which respectively resulted in the IC_{50} values of ~8.6 and 14.2 μg/mL at 48 h (Table 2). Furthermore, the light microscopic visualization illustrated that the treated cells displayed distinct morphologic alterations in comparison with the normal untreated cells in the appearance and the number of cells (Fig. 3).

*****Fig. 2*****

Fig. 3

Table 2

3.4. DAPI staining assay and AO/EB staining assay

Due to the direct interaction of plant-derived cytotoxic compounds with the cellular compartments, we expected to see some inadvertent biological alterations such as chromatin remodeling and detrimental impacts in cell membrane and nucleus in the treated cells. There are a number of investigations which have used DAPI staining and AO/EB assays to study the cellular impacts of natural products or synthetic compounds.[20, 21]In this investigation to reveal the cytotoxicity of the compounds, DAPI staining and AO/EB assays were utilized to assess possible remodeling of chromatin and nuclear fragmentation. Throughout these techniques, a significant nuclear fragmentation and chromatin condensation were observed in the MCF-7 cells treated with the compounds (**1**) and (**2**).

Fig. 3 represents the fluorescence microscopy micrographs of the DAPI-stained cells after exposure to 20 µg/mL of (**1**) and (**2**), as well as 5% DMSO (positive control).[22, 23]. It seems that the apoptotic cells are principally detected in the positive control, as well as compounds (**1**) and (**2**) treated cells. All treatments caused a statistically significant nucleus fragmentation and condensation in the chromatin and DNA within the treated cells, nevertheless their morphology did not altered in the untreated control cells.[24]

We also surveyed the viability of the treated cells by staining the cells with the fluorochromes AO/EB (Fig. 4). Live cells are not permeable to EB, yet permeable to AO. Hence, in the viable cells the interaction of AO dye with the DNA can produce green nuclear fluorescence. As shown in Fig. 4, the apoptotic cells revealed yellow chromatin in fragmented and condensed nucleus

often with cell membrane, however the necrotic cells appeared to have red nucleus, indicative to an interaction of EB dye with DNA in damaged cells. Treatment with (**1**) and (**2**) compounds (20 μg/mL) for 24 h appeared to increase the percentage of nonviable cells. Compound (**2**) considerably increased the number of apoptotic cells in the MCF-7 cells (Plane B). However, in the case of compound (**1**), markedly higher levels of necrosis were observed as compared to the untreated control cells.

*****Fig. 3*****

*****Fig. 4*****

3.5. Cell cycle analysis

Cell cycle arrest analysis also displayed the interaction of the compounds with DNA. Any cleavage in the chromosome at the inter-nucleosomal sites might lead to the activation of proteins that contributed in the regulation of the checkpoints in the cell cycle. It should be noted that the cell cycle arrest has already been reported as the main biochemical signs of the apoptotic cell death. [25] In order to test whether the isolated compounds can cause cell cycle arrest, we used propidium iodide (PI) for the staining double strand DNA whose levels are elevated in G_0/G_1 and G_2/M. We followed sub-G_0 population of the cells representing the fragmented ds DNA and condensed chromatin as the sign for occurrence of apoptosis. We compared the effects of (**1**) and (**2**) compounds in the treated cells in comparison with the untreated cells. Both compounds (**1**) and (**2**) appeared to exhibit similar patterns of cell cycle arrest. The effects of the compounds on the cell cycle modulation are shown in Fig. 5. The compound (**1**) exhibited a higher toxicity in cell viability assay, however the count of cells with fragmented DNA was slightly lower than that of the compound (**2**). Therefore, we postulate that the compounds could induce pyknosis and

karyopyknosis, which are the irreversible chromatin condensation and ds DNA strand breakages in the nucleus undergoing apoptosis[26] or necrosis.[27] The cells treated with compound (**2**) seemed to beassociated with a sharp sub-G_1 apoptotic peak (Fig. 5C), which may confer compound (**2**) to be an apoptosis promoting entity in the cells. Similarly, the compound (**1**) treated cells were found to cause a sub-G_1 peak in the MCF-7 cells, even though the cell population count seemed to be subordinated in association with a marked reduction of the sub-G_1 peak.

*****Fig. 5*****

3.6. Apoptosis detection using annexin V staining

Specific staining, using annexin V-FITC/PI flow cytometry, was performed to differentiate the necrotic cells form the apoptotic cells. It should be pointed out that annexin V is a cellular protein with a high affinity for phosphatidylserine (Ptd-L-Ser) in the presence of calcium ion, which identifies the alteration of Ptd-L-Ser on the outer leaflet of the plasma membrane as an early distinctive of apoptotic cells when labeled with a fluorescent probe.[28, 29] In our experiments, the FITC-labeled annexin V flow cytometry analyses confirmed the occurrence of apoptosis stages in the MCF-7 cells treated with compounds (**2**) (Fig. 6). These results revealed that more than 30% of (**2**)-treated cells underwent the apoptotic stage, while 2% of the cells underwent the necrotic stage after 24 h (Fig. 6). The results obtained from FACScalibur disclosed that the compound (**2**) could cause cell death, in large part because of the activation of apoptosis pathway(s).We also speculate that compound (**2**) may have pro-apoptotic properties in the treated dosage, and cell death prompted by the compound may be associated with the activation of apoptosis pathways similar to previous reports.[30] These data enabled us to distinguish the apoptotic cells from the necrotic and/or living cells.[31]

Fig. 6

3.7. Quantitative Real-Time PCR

Finally, we looked at various gene expression profiles known to be involved in apoptosis, in which the death signals are afforded after a chemical treatment in the cells directing to liberation of mitochondrial factors such as small mitochondria-derived activator of caspases (SMACs) into the cytosol.[32, 33] The intracellular apoptotic pathway can be regulated with the help of intracellular signals, which puts forward the cell in programmed death. An alteration in the permeability of the mitochondrial membrane can obligate the apoptotic proteins to release into the cell. It seems that some pores known as the mitochondrial outer membrane permeabilization pores (MACs) can control the permeability of the membrane to the apoptotic proteins. Proteins belonging to the Bcl-2 family can control the MACs.[34] The activated Bax protein (Bcl-2–associated X protein) dimerizes in the mitochondrial membrane. This dimerization stimulates the MAC pore development, causing apoptotic leakage of proteins into the cytosol. In contrast, the proteins Bcl-2 and Mcl-1 can inhibit the MAC creation, suppressing the release of apoptotic proteins into the cell.[35] The SMACs can bind to the inhibitors of apoptosis (IAP), which activates caspases in the cell.[36] Caspases are enzymes that can damage intracellular proteins, which finally leads to the entire cell death. In this study, we studied the expression of some of these genes (*Bcl-2, Akt, Caspase 9* and *Bax*) and found a significant regulation in the gene expression profile of the treated cells with compound (**2**) after 24 h. As illustrated in Fig. 7, the expression of *Caspase 9* gene was not significantly changed by the compound (**2**). Moreover, the expression of *Akt* and *Bcl-2* genes were significantly down-regulated in comparison with the untreated MCF-7 cells.

However, there was a significant up-regulation in the *Bax* gene (*Akt*'s downstream gene) in the cells treated with the compound (**2**) after 24 h, which was not amazing due to the down-regulation of *Akt.* We speculate that the initiation of apoptosis in the treated cells by ortho-diacetate aethiopinone may be through PI3K/AKT pathway that is a known pathway involves in breast cancer.[37]

*****Fig. 7*****

4. Conclusion

Taken all, the current study outcomes showed that the two abietane diterpene extracted from *S. sahendica* inhibited the growth of MCF-7 cells in a time and dose-dependent manner and persuaded cytotoxicity via inducing apoptosis and necrosis. It was found that ketoethiopinone (**1**) and ortho-diacetate aethiopinone (**2**) are able to inhibit the proliferation of the MCF-7 cells by stimulating apoptosis via DNA and chromatin fragmentation. We also showed the incidence of early/late stages of apoptosis within MCF-7 cells treated with compound (**2**) by FITC-labeled annexin V flow cytometry and nuclear staining assays. Furthermore, using the cell cycle arrest and DNA fragmentation assays, significant fragmentation of DNA were found in the treated cells with compound (**2**). Technically, significant decreases in *Akt, Bcl-2* expressions and an increase in *Bax* expression may lead us towards possible involvement of the PI3K/AKT pathway in the modulation of MCF-7 cells proliferation by the compound (**2**). In conclusion, all the data presented pinpointed that ortho-diacetate aethiopinone is able to elicit profound cytotoxic impacts in the cancerous cells. We envision this compound as potential candidate for further translational/clinical studies that may provide a novel chemotherapy agent to tackle the breast cancer and perhaps other types of solid tumors.

Abbreviations

NMR	Nuclear magnetic resonance
MCF-7	Michigan cancer foundation – 7
DMSO	Dimethyl sulfoxide
MTT	3-[4, 5-dimethylthiazol-2-yl]-2, 5-diphenyltetrazolium bromide
DAPI	4',6-diamidino-2-phenylindole
PBS	Phosphate buffered saline
FBS	Fetal bovine serum
RT-PCR	Reverse transcription and real time polymerase chain reactions
MMLV-rt	Moloney murine leukemia virus reverse-transcriptase

Acknowledgement

This work was supported by the Research Center for Pharmaceutical Nanotechnology (RCPN) at Tabriz University of Medical Sciences (grant No: 90011, which is a part of PhD thesis No: 90/011/101/1).

Disclosure of interest

The authors declare no conflicts of interest concerning this article.

References

1. D. S. Alberts, K. S. Griffith, G. E. Goodman, T. S. Herman and E. Murray, *Cancer chemotherapy and pharmacology*, 1980, **5**, 11-15.
2. M. Eskandani, J. Abdolalizadeh, H. Hamishehkar, H. Nazemiyeh and J. Barar, *Fitoterapia*, 2015, **101**, 1-11.
3. M. Fronza, R. Murillo, S. Ślusarczyk, M. Adams, M. Hamburger, B. Heinzmann, S. Laufer and I. Merfort, *Bioorganic & medicinal chemistry*, 2011, **19**, 4876-4881.
4. M. Alikhani1, A. Rezwani, E. Rakhshani and S. Madani, in *Journal of Entomological Research*, 2010, vol. 2, pp. 7-16.
5. F. Lotfipour, M. Samiee and H. Nazemiyeh, *Pharmaceutical Sciences*, 2007, **1**, 3.
6. F. M. Moghaddam, B. Zaynizadeh and P. Rüedi, *Phytochemistry*, 1995, **39**, 715-716.
7. A. R. Jassbi, M. Mehrdad, F. Eghtesadi, S. N. Ebrahimi and I. T. Baldwin, *Chemistry & biodiversity*, 2006, **3**, 916-922.
8. F. M. Moghaddam, M. M. Farimani, M. Seirafi, S. Taheri, H. R. Khavasi, J. Sendker, P. Proksch, V. Wray and R. Edrada, *Journal of natural products*, 2010, **73**, 1601-1605.
9. M. Heidari Majd, D. Asgari, J. Barar, H. Valizadeh, V. Kafil, G. Coukos and Y. Omidi, *Journal of drug targeting*, 2013, 1-13.

467 10. M. Eskandani and H. Nazemiyeh, *European journal of pharmaceutical sciences*, 2014,
468 **59**, 49-57.
469 11. S. Vandghanooni, A. Forouharmehr, M. Eskandani, A. Barzegari, V. Kafil, S. Kashanian
470 and J. Ezzati Nazhad Dolatabadi, *DNA and Cell Biology*, 2013.
471 12. M. Eskandani, H. Hamishehkar and J. Ezzati Nazhad Dolatabadi, *Food chemistry*, 2014,
472 **153**, 315-320.
473 13. M. Deepaa, T. Sureshkumara, P. K. Satheeshkumara and S. Priya, *Chemico-Biological*
474 *Interactions*, 2012.
475 14. V. Kafil and Y. Omidi, *BioImpacts*, 2011, **1**, 23-30.
476 15. M. Eskandani, H. Hamishehkar and J. Ezzati Nazhad Dolatabadi, *DNA and Cell Biology*,
477 2013, **32**, 498-503.
478 16. S. Vandghanooni, M. Eskandani, V. Montazeri, M. Halimi, E. Babaei and M. A. Feizi,
479 *Journal of cancer research and therapeutics*, 2011, **7**, 325-330.
480 17. M. W. Pfaffl, *Nucleic acids research*, 2001, **29**, e45-e45.
481 18. M. T. Boya and S. Valverde, *Phytochemistry*, 1981, **20**, 1367-1368.
482 19. A. Michavila, M. C. De La Torre and B. Rodríguez, *Phytochemistry*, 1986, **25**, 1935-
483 1937.
484 20. S. Kandekar, R. Preet, M. Kashyap, M. U. Renu Prasad, P. Mohapatra, D. Das, S. R.
485 Satapathy, S. Siddharth, V. Jain, M. Choudhuri, C. N. Kundu, S. K. Guchhait and P. V.
486 Bharatam, *ChemMedChem*, 2013, **8**, 1873-1884.
487 21. T. W. Tan, H. R. Tsai, H. F. Lu, H. L. Lin, M. F. Tsou, Y. T. Lin, H. Y. Tsai, Y. F. Chen
488 and J. G. Chung, *Anticancer research*, 2006, **26**, 4361-4371.

22. C. Yuan, J. Gao, J. Guo, L. Bai, C. Marshall, Z. Cai, L. Wang and M. Xiao, *PLoS ONE*, 2014, **9**, e107447.

23. J. L. Hanslick, K. Lau, K. K. Noguchi, J. W. Olney, C. F. Zorumski, S. Mennerick and N. B. Farber, *Neurobiology of disease*, 2009, **34**, 1-10.

24. F. Madeo, E. Fröhlich and K.-U. Fröhlich, *The Journal of cell biology*, 1997, **139**, 729-734.

25. G. I. Evan and K. H. Vousden, *Nature*, 2001, **411**, 342-348.

26. G. Kroemer, L. Galluzzi, P. Vandenabeele, J. Abrams, E. S. Alnemri, E. Baehrecke, M. Blagosklonny, W. El-Deiry, P. Golstein and D. Green, *Cell Death & Differentiation*, 2008, **16**, 3-11.

27. Z. Darzynkiewicz, G. Juan, X. Li, W. Gorczyca, T. Murakami and F. Traganos, *Cytometry*, 1997, **27**, 1-20.

28. H. Hamishehkar, S. Khani, S. Kashanian, J. Ezzati Nazhad Dolatabadi and M. Eskandani, *Drug and chemical toxicology*, 2014, **37**, 241-246.

29. M. Eskandani, E. Dadizadeh, H. Hamishehkar, H. Nazemiyeh and J. Barar, *Bioimpacts*, 2014, **4**, 191-198.

30. S. B. Bratton and G. S. Salvesen, *Journal of cell science*, 2010, **123**, 3209-3214.

31. K. S. Ravichandran, *Immunity*, 2011, **35**, 445-455.

32. M. J. Koziol and J. B. Gurdon, *Biochemistry Research International*, 2012, **2012**.

33. M. MacFarlane, W. Merrison, S. B. Bratton and G. M. Cohen, *Journal of Biological Chemistry*, 2002, **277**, 36611-36616.

34. L. M. Dejean, S. Martinez-Caballero, S. Manon and K. W. Kinnally, *Biochimica et Biophysica Acta (BBA)-Molecular Basis of Disease*, 2006, **1762**, 191-201.

35. F. Llambi and D. R. Green, *Current opinion in genetics & development*, 2011, **21**, 12-20.

36. S. W. Fesik and Y. Shi, *Science*, 2001, **294**, 1477-1478.

37. M. Osaki, M. a. Oshimura and H. Ito, *Apoptosis*, 2004, **9**, 667-676.

Figures legend

Fig. 1 Structures of the isolated compounds from the n-Hexane extract of *S. sahendica* roots.

Fig.2 In vitro cytotoxicity of A) ketoaethiopinone (**1**), B) ortho-diacetate aethipinone (**2**) extracted from S. sahendica and C) doxorubicin (Dox) in MCF-7 cells. Data represent cell viability of cells exposed to the demonstrated concentration (5-100 µg/mL) for 24, 48 and 72 hr. Significant differences in cell viability were observed after different times with 10 µg/ml of ketoaethiopinone (1) and with 10 and 20 µg/ml of ortho-diacetate aethipinone (2).

Fig. 3 Light microscopy and DAPI staining for nuclei condensation and fragmentation assessment (magnification 200×): A and B) Untreated control MCF-7 displaying normal epithelial morphology, C and D) 24 h after exposure to 20 µg/mL of ketoaethiopinone (**1**), E and F) 24 h after exposure to 20 µg/mL of ortho-diacetate aethiopinone (**2**), and G and H) 24 h after exposure to the 5% DMSO as a positive control. Control cells possess normal nuclear morphology, whereas apoptotic cells showed clear morphological changes such as nuclear fragmentation and chromatin condensation (represented by white arrows).

Fig. 4 Apoptotic morphological variations of MCF-7 cells identified with AO/EB staining and observed under fluorescence microscope (magnification 200×): UT) Untreated control MCF-7 displaying normal epithelial morphology, A) 24 h after exposure to 20 µg/mL of ketoaethiopinone (**1**), B) 24 h after exposure to 20 µg/mL of ortho-diacetate aethiopinone (**2**), C) 24 h after exposure to the 5% DMSO as a positive control. The viable cell possess unchanged green nuclear, apoptotic cells have bright green-orange areas of fragmented or condensed chromatin in the nuclear, and the necrotic cells have uniform bright red nuclear. White empty arrows show the apoptotic cells and white fill arrows indicate the necrotic cells.

Fig. 5 Cell cycle analysis: A) MCF-7 cells treated with 5% DMSO as positive control, B) 20 µg/mL of ketoaethiopinone (**1**), C) MCF-7 cells treated with 20 µg/mL of ortho-diacetate aethiopinone (**2**) for 24 h, analyzed by FACS flow cytometry for the distribution of cells in different phases of cell cycle.

Fig. 6 FITC-labeled Annexin V flow cytometric detection of apoptosis in MCF-7 cells: A) MCF-7 ells treated with 20 µg/mL of ortho-diacetate aethiopinone (**2**) for 24 h, B) MCF-7 untreated cells for 24 h, and C) 24 h after exposure to the 5% DMSO as a positive control. Considerable late stages of apoptosis were detected in the cells treated with ortho-diacetate aethiopinone compared to untreated cells ($p<0.05$).

Fig. 7 Gene expression ratios of Akt, Caspase 9, Bcl-2 and Bax in the treated cells with ortho-diacetate aethiopinone, untreated control MCF-7 cells. * represent significant differences between defined group ($P<0.05$)

Table 1 Primer's sequence for the genes studied.

Primer	Primer sequence	Gene Bank accession no	Annealing (Tm)
18S rRNA	F: 5′-CGATGCGGCGGCGTTATTC-3′ R: 5′-TCTGTCAATCCTGTCCGTGTCC-3′	NR_003286.1	61
Bcl-2	F: 5′-CATCAGGAAGGCTAGAGTTACC-3′ R: 5′-CAGACATTCGGAGACCACAC-3′	NM_000633.2	56
Caspase 9	F: 5′- TGCTGCGTGGTGGTCATTCTC-3′ R: 5′- CCGACACAGGGCATCCATCTG-3′	NM_001229.2	62
Akt	F: 5'- CGCAGTGCCAGCTGATGAAG -3' R: 5'- GTCCATCTCCTCCTCCTCCTG -3'	NM_005163.2	62
Bax	F: 5'-AAGCTGAGCGAGTGTCTCAAGCGC-3' R: 5'-TCCCGCCACAAAGATGGTCACG-3'	NR_027882	53

Table 2 IC_{50} values for Ketoethiopinone (**1**) and ortho-diacetate aethiopinone (**2**).

Exposure time	Ketoethiopinone (1)	ortho-diacetate aethiopinone (2)	Doxorubicin
24 h	10 μg/mL	21 μg/mL	70 μg/mL
48 h	8.6 μg/mL	14.2 μg/mL	42 μg/mL
72 h	5.9 μg/mL	7.4 μg/mL	38 μg/mL

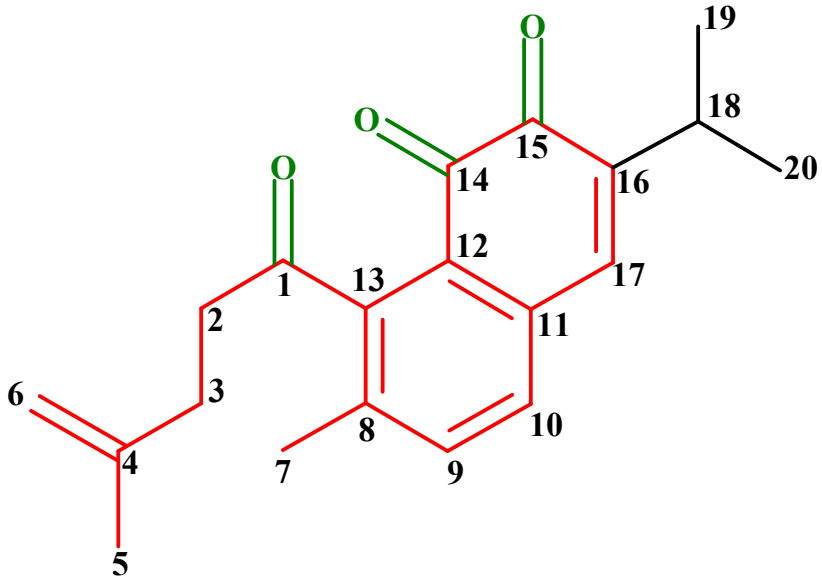

Ketoethiopinone (**1**)

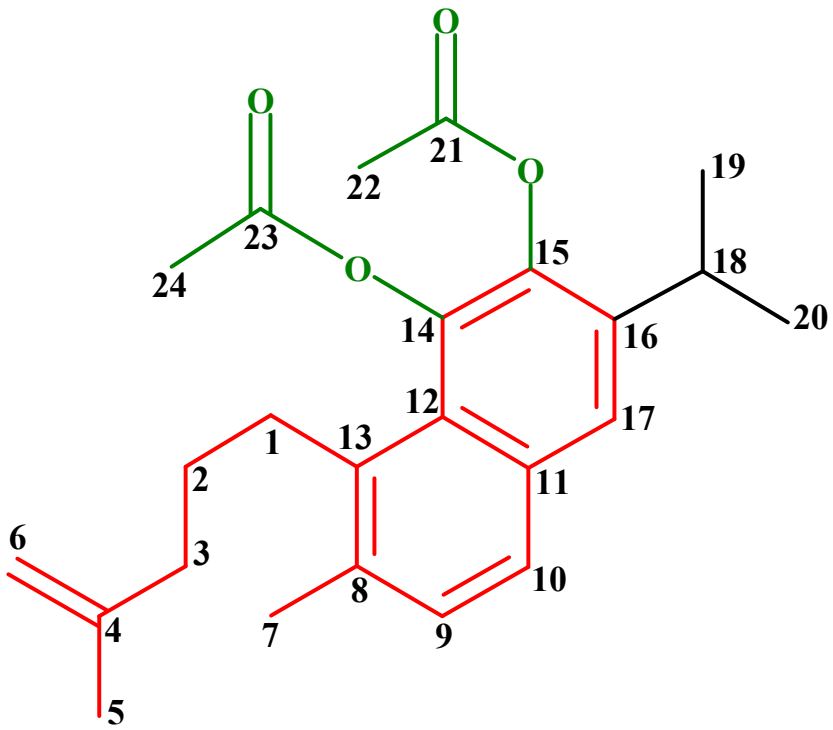

Ortho-diacetate aethiopinone (**2**)

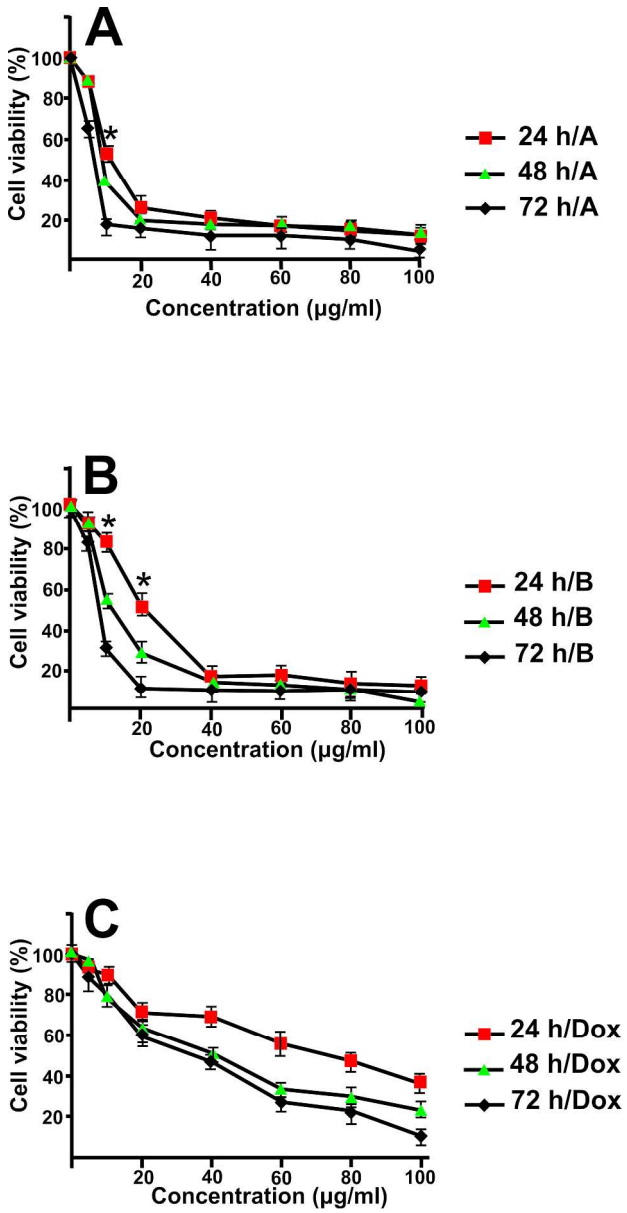

Fig.2 In vitro cytotoxicity of A) ketoaethiopinone (1), B) ortho-diacetate aethipinone (2) extracted from S. sahendica and C) doxorubicin (Dox) in MCF-7 cells. Data represent cell viability of cells exposed to the demonstrated concentration (5-100 µg/mL) for 24, 48 and 72 hr. Significant differences in cell viability were observed after different times with 10 µg/ml of ketoaethiopinone (1) and with 10 and 20 µg/ml of ortho-diacetate aethipinone (2).
137x268mm (600 x 600 DPI)

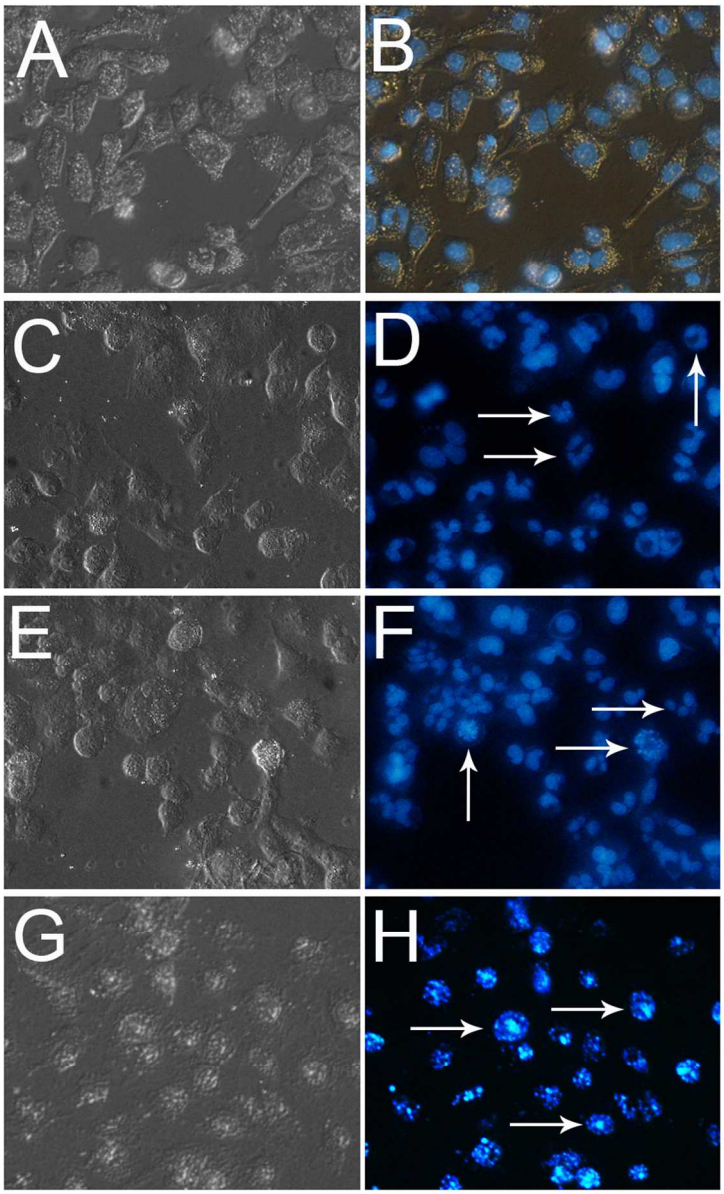

Fig. 3 Light microscopy and DAPI staining for nuclei condensation and fragmentation assessment (magnification 200×): A and B) Untreated control MCF-7 displaying normal epithelial morphology, C and D) 24 h after exposure to 20 μg/mL of ketoaethiopinone (1), E and F) 24 h after exposure to 20 μg/mL of ortho-diacetate aethiopinone (2), and G and H) 24 h after exposure to the 5% DMSO as a positive control. Control cells possess normal nuclear morphology, whereas apoptotic cells showed clear morphological changes such as nuclear fragmentation and chromatin condensation (represented by white arrows).
85x140mm (300 x 300 DPI)

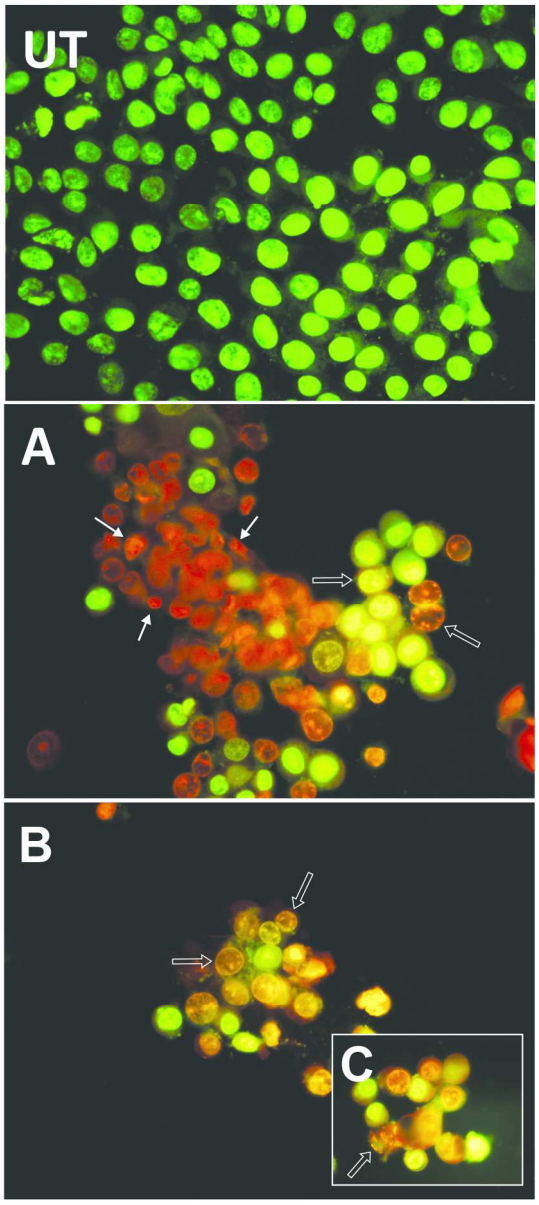

Fig. 4 Apoptotic morphological variations of MCF-7 cells identified with AO/EB staining and observed under fluorescence microscope (magnification 200×): UT) Untreated control MCF-7 displaying normal epithelial morphology, A) 24 h after exposure to 20 μg/mL of ketoaethiopinone (1), B) 24 h after exposure to 20 μg/mL of ortho-diacetate aethiopinone (2), C) 24 h after exposure to the 5% DMSO as a positive control. The viable cell possess unchanged green nuclear, apoptotic cells have bright green-orange areas of fragmented or condensed chromatin in the nuclear, and the necrotic cells have uniform bright red nuclear. White empty arrows show the apoptotic cells and white fill arrows indicate the necrotic cells.
92x207mm (300 x 300 DPI)

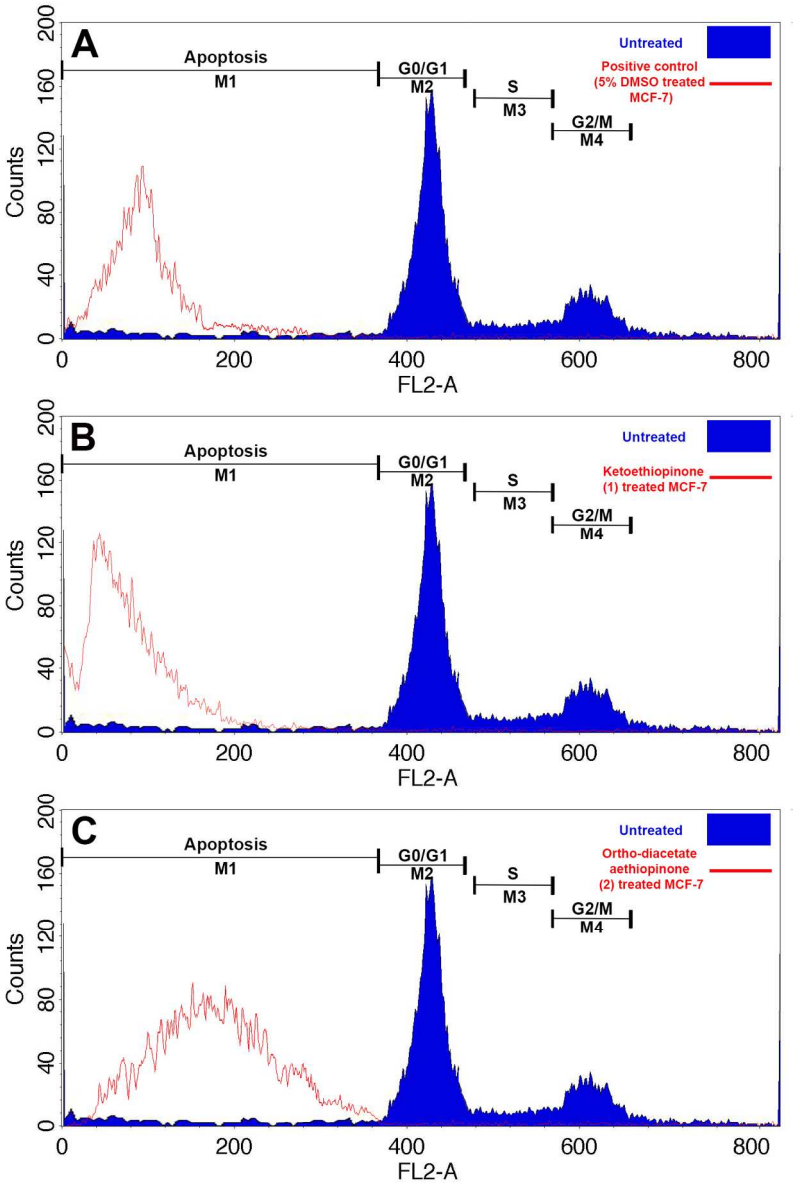

Fig. 5 Cell cycle analysis: A) MCF-7 cells treated with 5% DMSO as positive control, B) 20 µg/mL of ketoaethiopinone (1), C) MCF-7 cells treated with 20 µg/mL of ortho-diacetate aethiopinone (2) for 24 h, analyzed by FACS flow cytometry for the distribution of cells in different phases of cell cycle.
129x198mm (300 x 300 DPI)

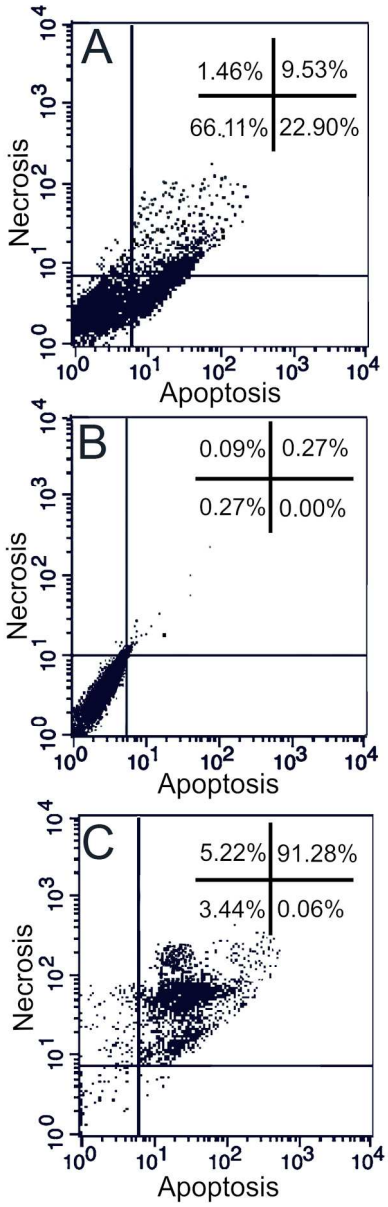

Fig. 6 FITC-labeled Annexin V flow cytometric detection of apoptosis in MCF-7 cells: A) MCF-7 ells treated with 20 μg/mL of ortho-diacetate aethiopinone (2) for 24 h, B) MCF-7 untreated cells for 24 h, and C) 24 h after exposure to the 5% DMSO as a positive control. Considerable late stages of apoptosis were detected in the cells treated with ortho-diacetate aethiopinone compared to untreated cells ($p<0.05$).
73x215mm (299 x 299 DPI)

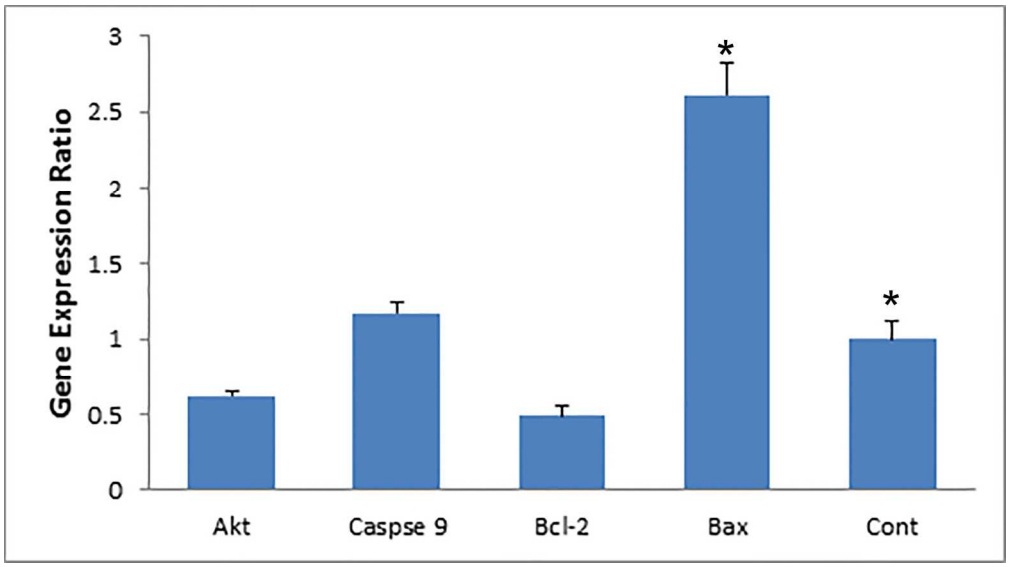

Fig. 7 Gene expression ratios of Akt, Caspase 9, Bcl-2 and Bax in the treated cells with ortho-diacetate aethiopinone, untreated control MCF-7 cells. * represent significant differences between defined group (P<0.05)

169x94mm (300 x 300 DPI)